Characterization of Geoinspired and Synthetic Chrysotile Nanotubes by Atomic Force Microscopy and Transmission Electron Microscopy

ARTICLE *in* ADVANCED FUNCTIONAL MATERIALS · SEPTEMBER 2007

Impact Factor: 11.81 · DOI: 10.1002/adfm.200700278

9 AUTHORS, INCLUDING:

Sidney R Cohen
Weizmann Institute of Science
175 PUBLICATIONS **4,869** CITATIONS
SEE PROFILE

Daniel Hanoch Wagner
Weizmann Institute of Science
266 PUBLICATIONS **12,377** CITATIONS
SEE PROFILE

Giorgio Lesci
LEBSC srl
57 PUBLICATIONS **772** CITATIONS
SEE PROFILE

Norberto Roveri
University of Bologna
194 PUBLICATIONS **4,889** CITATIONS
SEE PROFILE

ADVANCED FUNCTIONAL MATERIALS

DOI: 10.1002/adfm.200700278

Characterization of Geoinspired and Synthetic Chrysotile Nanotubes by Atomic Force Microscopy and Transmission Electron Microscopy**

By *Silvia Piperno*, *Ifat Kaplan-Ashiri*, *Sidney R. Cohen*, *Ronit Popovitz-Biro*, *H. Daniel Wagner*, *Reshef Tenne*,* *Elisabetta Foresti*, *Isidoro Giorgio Lesci*, and *Norberto Roveri*

Geoinspired synthetic chrysotile nanotubes both stoichiometric and 0.67 wt % Fe doped were characterized by transmission electron microscopy and electron diffraction. Bending tests of the synthetic chrysotile nanotubes were performed using the atomic force microscope. The nanotubes were found to exhibit elastic behaviour at small deformations (below ca. 20 nm). Young's modulus values of (159±125) GPa and (279±260) GPa were obtained from the force-deflection curves using the bending equation for a clamped beam under a concentrated load, for the stoichiometric and the Fe doped chrysotile nanotubes, respectively. The structural modifications induced by Fe doping altered the mechanical properties, with an apparent dependence of the latter on the number of constituting walls of the nanotubes.

1. Introduction

The mechanics of nanoscale materials is of great interest for both future applications and fundamental science. Materials with reduced size and dimensionality such as nanotubes, nanofibres or nanowires often present exceptional properties compared to those of the corresponding macroscopic material.[1–4] Studies on the mechanics of nanomaterials have indicated that in general the elastic properties of the nanotube, such as the Young's modulus, are not dramatically affected by the presence of defects and the tubular morphology and are therefore not different from the bulk material.[5,6] Contrarily, mechanical properties which go beyond the linear regime of the force-deformation curve and are measured under much higher loads, such as the yield strength and strain are non-linear in nature, and may differ markedly from the values of the bulk material. The reason for this discrepancy is the large concentration of defects in bulk materials. Therefore bulk materials yield under much lower loads than would be anticipated based on the strength of their chemical bonds alone. Thus, nanotubes of carbon[1] and WS_2[4] under tension deform elastically for strain values of 10 % and above, whereas in the bulk form these materials fail at much smaller strain values, particularly along the longitudinal *c*-axis. Furthermore, carbon and WS_2 nanotubes[4] as well as gold nanowires[3] show very high strengths compared to their bulk form and to other high strength materials.

Although a lot of progress has been made in developing tools for measurement of the characteristics of nanoscale materials, it is still quite a challenging task. A most demanding task is trying to understand the effect of strain on the atomic structure of the nanotube or nanowire, which has been rarely demonstrated, by, e.g., loading a nanotube (nanowire) in a high resolution transmission electron microscope.[7–10] Imaging tools like scanning electron microscopy (SEM) and scanning force microscopy can be transformed into measurement tools and play a central role in the field of experimental nanomechanics[1,4,6,11–13]

Point load bending tests of nanotubes or nanowires are simpler to perform compared to other mechanical tests. Detailed description and analysis of beam bending under various conditions appear in the literature,[14,15] including the cases of homogeneous and composite materials. The bending deflection of a nanotube viewed as a clamped isotropic beam under a concentrated load is described by the equation:[3]

$$\delta = \frac{FL^3}{192EI} \quad (1)$$

where δ is the nanotube deflection, F is the applied force, L is the suspended nanotube length, E is Young's modulus. I is the

[*] Prof. R. Tenne, I. Kaplan-Ashiri, Prof. H. D. Wagner
Department of Material and Interfaces, Weizmann Institute of Science
Rehovot 76100 (Israel)
E-mail: reshef.tenne@weizmann.ac.il
Dr. S. Piperno
INFM-CNR and Department of Physics, University of L'Aquila
Via Vetoio, 67010 Coppito, L'Aquila (Italy)
Dr. S. R. Cohen, Dr. R. Popovitz-Biro
Chemical Research Support, Weizmann Institute of Science
Rehovot 76100 (Israel)
Dr. E. Foresti, Dr. I. G. Lesci, Prof. N. Roveri
Department of Chemistry "G. Ciamician"
Alma Mater Studiorum University of Bologna
Via Selmi 2, 40126, Bologna (Italy)

[**] This work was supported by the Israel Science Foundation; the Minerva Foundation (Munich) and the GMJ Schmidt Centre for Supramolecular Architectures. R.T. is the director of the Helen and Martin Kimmel Centre for Nanoscale Science and holds the Drake Family Professorial Chair for Nanotechnology. H.D.W. is the recipient of the Livio Norzi Professorial Chair. The Authors are grateful to Prof. Sandro Santucci, the Head of the Physics Department of L'Aquila University, for helpful discussions.

second moment of area (for a cylindrical nanotube: $I = \pi/4(r_{out}^4 - r_{in}^4)$ where r_{out} and r_{in} are the outer and inner radii of the nanotube, respectively). The stresses induced in a bending experiment include tension, compression and shear. In the case of isotropic materials with long enough span the contribution of shear to the total deflection can be ignored.[16,17] Bending tests made on a variety of nanoscale systems, including carbon,[18] MoS_2[19] and WS_2 nanotubes[20] as well as gold nanowires[3] revealed that the bending mechanism is strongly dependent on the system studied. Gold nanowires (which were considered as isotropic material) exhibit elastic-plastic bending deformation.[3] The nanowire plasticity was dominated by strain-hardening and demonstrated that dislocation motion and pile-up can be operative down to diameters of 40 nm. Bending tests of ropes of single wall carbon[18] and MoS_2[19] nanotubes revealed a unique bending mechanism which includes a significant contribution of shearing to the total deflection. The shearing deformation originated from the weak interactions between the nanotubes in the ropes, thus promoting sliding of the nanotubes with respect to each other. Here, Young's modulus values of 1 TPa and 120 GPa were obtained for carbon and MoS_2 nanotubes, respectively. For carbon ropes, this value is in good agreement with that of graphite. Ropes of carbon nanotubes were also analysed as elastic strings, with the tension proportional to their elongation.[21] Another unique bending mechanism was also observed for individual multiwall WS_2 nanotubes.[20] For these nanotubes a significant shear deformation was observed as well, which originated from the telescopic sliding of the molecular layers with respect to each other within the nanotube itself. Since nanotubes and ropes are anisotropic systems, it is reasonable to observe dominant shear deformation as long as the system is free of defects.

The mineral chrysotile, $Mg_3Si_2O_5(OH)_4$, consists of sheets of tetrahedral (T) silica in a pseudohexagonal network joined to a brucite layer in which Mg is in octahedral (O) coordination chemically bound to the apical oxygen of the SiO_4 layer and additional hydroxyl groups (see Fig. 1). The mismatch between the smaller lateral dimension of the SiO_4 sheet with respect to the $Mg(OH)_2$ layer is accommodated by the OT layers winding concentrically or spirally around the x axis into a tubular structure of about 22–27 nm in diameter.[22–24] The nanoscrolls possess hollow cores with a diameter of about 5–8 nm. The elastic energy of bending rises sharply with diminishing diameter of the nanotube/nanoscroll, thereby preventing the formation of structures of a smaller diameter[25] (see Fig. 2). The morphology and structure of naturally occurring chrysotile fibers and tubes vary considerably according to the different mined ores and even from sample to sample from the same site.[23] Naturally occurring chrysotile fibers (nanotubes) may contain different amounts of chrysotile polytypes and usually show an intimate intergrowth of chrysotile polymorphs such as lizardite and antigorite and other minerals.[20] Also, natural mineral fibres are contaminated with trace metals such as Fe, Al and Ni, which can replace Mg and Si atoms, usually developing structural defects.[26] Recently, hydrothermal synthesis of chrysotile nanotubes has been reported.[27,28] Figure 2 presents the (open-ended) tip of one such nanotube with the OT layers clearly revealed. Synthetic chrysotile nanotubes may find various applications in the burgeoning field of nanotechnology.[27] Most interestingly, in contrast with the naturally occurring nanotubes, the synthetic ones were found to be non-toxic.[29] The chrysotile nanotubes can serve as a platform for encapsulation of various nanowires in their hollow core, offering opportunities to prepare innovative inorganic quantum wires with tailored morphological, structural and mechanical properties.[29,30] Additionally, doping the nanotubes with different metals, like iron, can offer an alternative route to vary their physico-chemical properties in a controlled fashion.[31] The inclusion of small amounts of Fe, which preferentially replaces Si in the chrysotile lattice leads to appreciable deterioration of the nanotube crystallinity.

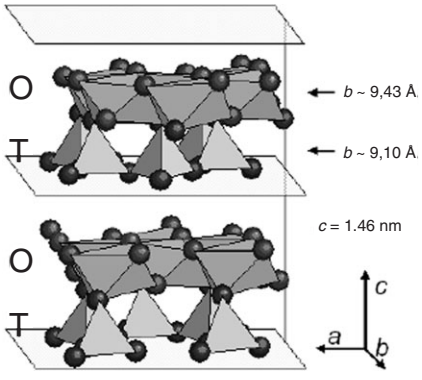

Figure 1. The lattice of chrysotile showing the incommensurate conformation between the smaller silica tetrahedra (light) and the sheet of darker $Mg(OH)_2$ octahedra.

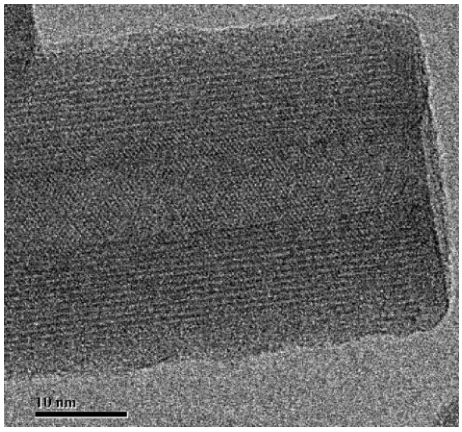

Figure 2. TEM image of the tip of a synthetic chrysotile nanotube. Note the open end of the nanotube and the amorphous coating.

In the present study bending tests of both stoichiometric chrysotile and Fe doped chrysotile nanotubes were conducted by means of lateral deflection in the atomic force microscope (AFM). The nanotubes demonstrated linear elastic deformation for small deflections. The Young's modulus of the nano-

ADVANCED FUNCTIONAL MATERIALS

tubes was determined from the force deflection curves by applying the bending equation.

2. Results and Discussion

Stoichiometric chrysotile nanotubes and Fe doped chrysotile nanotubes were synthesized and then characterized by transmission electron microscope (TEM). The results of the TEM analysis of the chrysotile nanotubes are presented in Figures 3–6. The stoichiometric chrysotile fibers which are shown in Figure 3A, demonstrate a hollow structure, with quite a uniform outer diameter ca. 35 nm and inner diameter 7–8 nm. The nanotubes are open ended and several hundred nanometer in length. The splitting in the electron diffraction pattern is a good evidence for the chirality of these nanotubes. Figure 4 presents a high magnification image of these nanotubes. Here (as well as in Fig. 6B for the doped nanotube) the layered

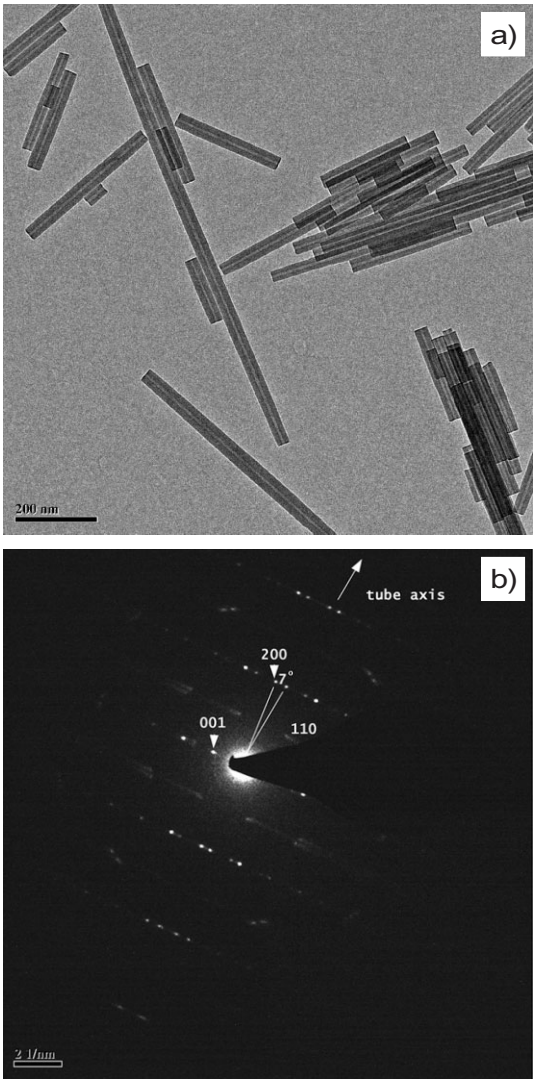

Figure 3. TEM analysis of stoichiometric chrysotile nanotubes, low magnification (a) and electron diffraction pattern (b).

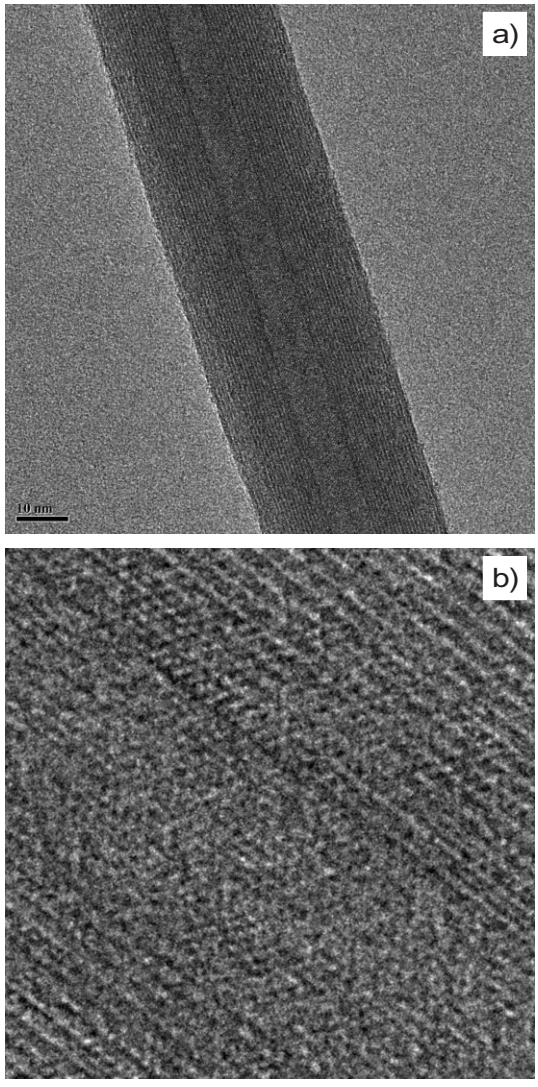

Figure 4. a,b) TEM images of a stoichiometric chrysotile nanotube.

structure can be seen very clearly; although the outermost part of the nanotube seems to be amorphous. Morphological differences can be seen in the Fe doped nanotubes. As seen in Figure 5a, the hollow structure with open ended tips was maintained, but the nanotubes form telescopic structures. The outer diameter range is 24–53 nm, with a similar inner diameter compared to the stoichiometric nanotubes. Also, in accordance with a previous study the Fe doped nanotubes seem to contain more structural defects as compared to the stoichiometric chrysotile nanotubes. Again the layered structure is clearly demonstrated in Figure 6a and b with the separate O and T layers discernable according to this HRTEM image.

Bending tests of the chrysotile nanotubes were conducted by loading a suspended nanotube (Fig. 7). The force-deflection (F-d) curves of both stoichiometric and Fe-doped chrysotile nanotubes are presented in Figure 8. The stoichiometric chrysotile nanotubes demonstrate linear elastic deformation to a maximal deflection of 20 nm. At 40 nm deflection, a non linear

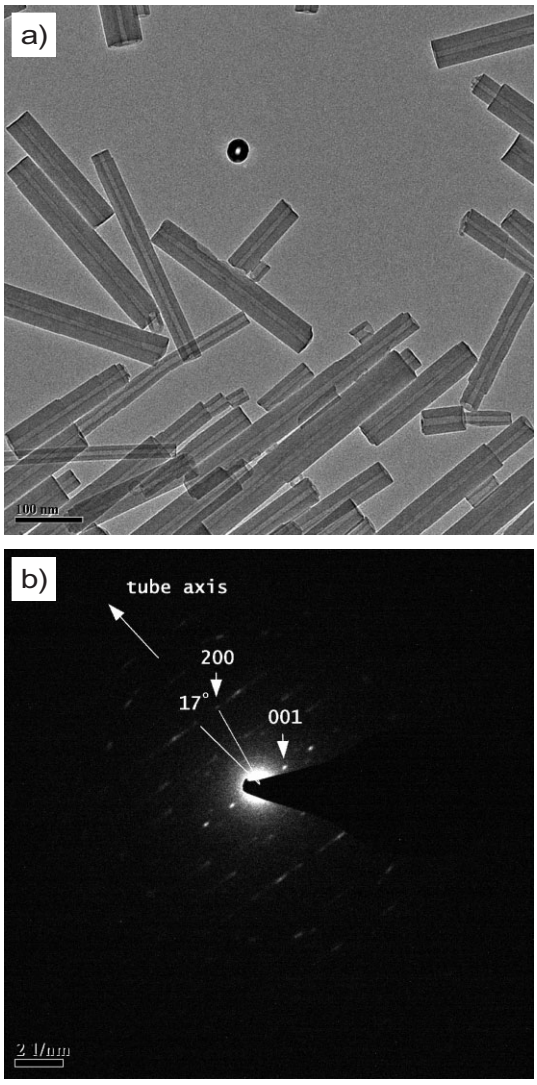

Figure 5. TEM analysis of Fe doped chrysotile nanotubes, low magnification image (a) and electron diffraction pattern showing the 17 degree chirality of the nanotube (b).

behavior is observed which may indicate the beginning of a plastic deformation. The Fe-doped chrysotile nanotubes demonstrate linear elastic deformation only for deflections less than 15 nm. At larger deflections an unusual behaviour is observed, which can be attributed to a weak contact between the nanotube and the GaAs substrate.

Some of the chrysotile nanotubes failed when they were deflected to 100–150 nm. The failure occurred at about 20 % strain for the stoichiometric and 25 % for the Fe doped chrysotile nanotubes. In some cases, fracture occurred in the middle of the nanotube and in others at the edge of the nanotube. The failure can be associated with a discontinuity in the force-deflection curve during loading and zeroing-out of the force during the unloading.

The Young's moduli of the chrysotile nanotubes were calculated according to the bending equation (Eq. 1) and are presented in Tables 1 and 2. The geometrical data of the nanotubes was obtained from SEM and AFM analysis. The average Young's modulus for the stoichiometric and the Fe-doped chry-

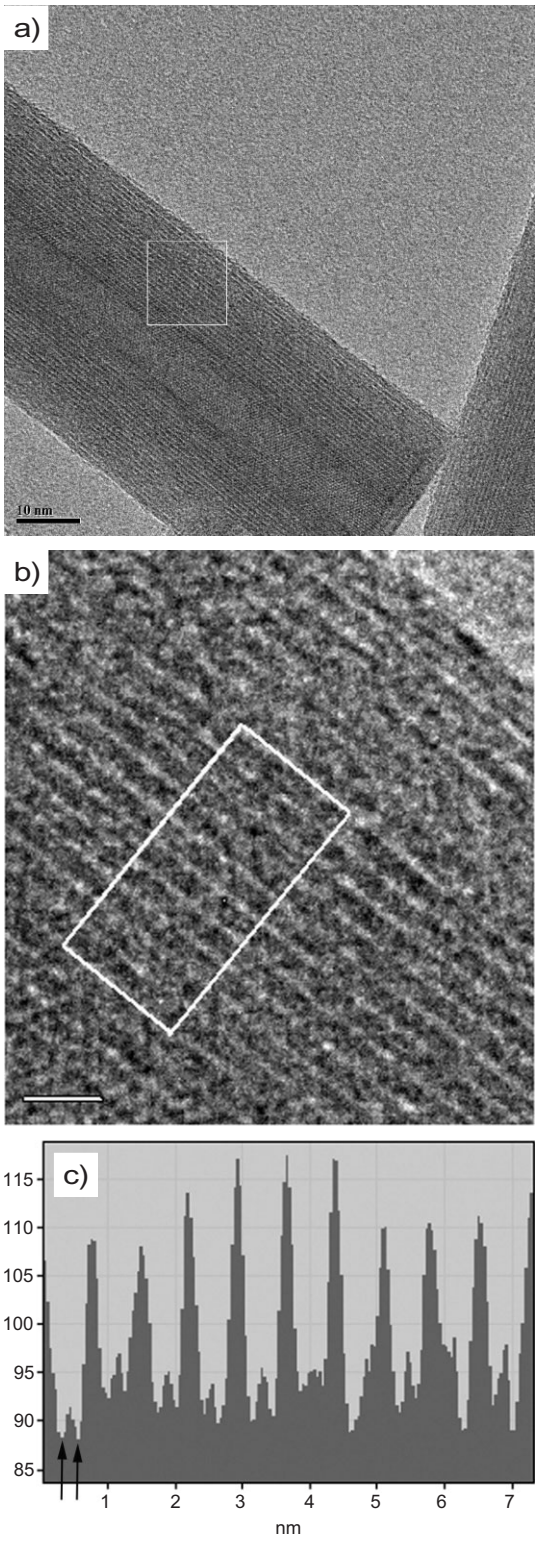

Figure 6. TEM image of Fe doped chrysotile nanotube (a) and magnification of the marked area (b). Line scan results are demonstrated in (c) and show a layer spacing ($c/2$) of 0.73 nm. The arrows in the line scan show the splitting of the lattice fringes, resolving the O and T sub-layers.

ADVANCED FUNCTIONAL MATERIALS

Table 1. Young's modulus for stoichiometric chrysotile nanotubes.

	Diameter [nm]	Length [nm]	Maximum deflection [nm]	Young's modulus(GPa) [1st]	Young's modulus(GPa) [2nd]
1	40	620	5	271	302
2	33	650	5	336	212
3	41	655	5	16	14
4	42	600	5	67	51
5	32.5	580	5	208	316
6	34	660	5	61	58

Table 2. Young's modulus for iron doped chrysotile nanotubes.

	Diameter [nm]	Length [nm]	Maximum deflection [nm]	Young's modulus(GPa) [1st]	Young's modulus(GPa) [2nd]
1	34	670	10	555	471
2	46	670	5		118
3	36	800	5		724
4	60	650	5	46	42
5	45	670	5	146	137

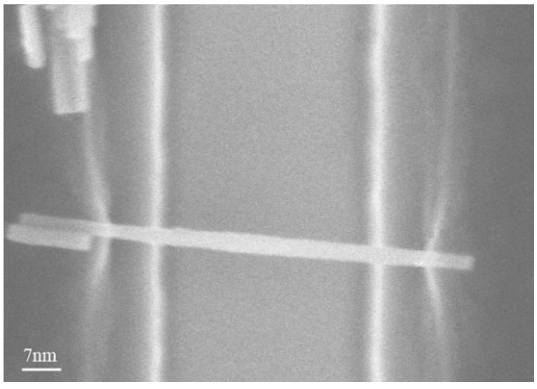

Figure 7. SEM picture of the chrysotile nanotubes doped with iron.

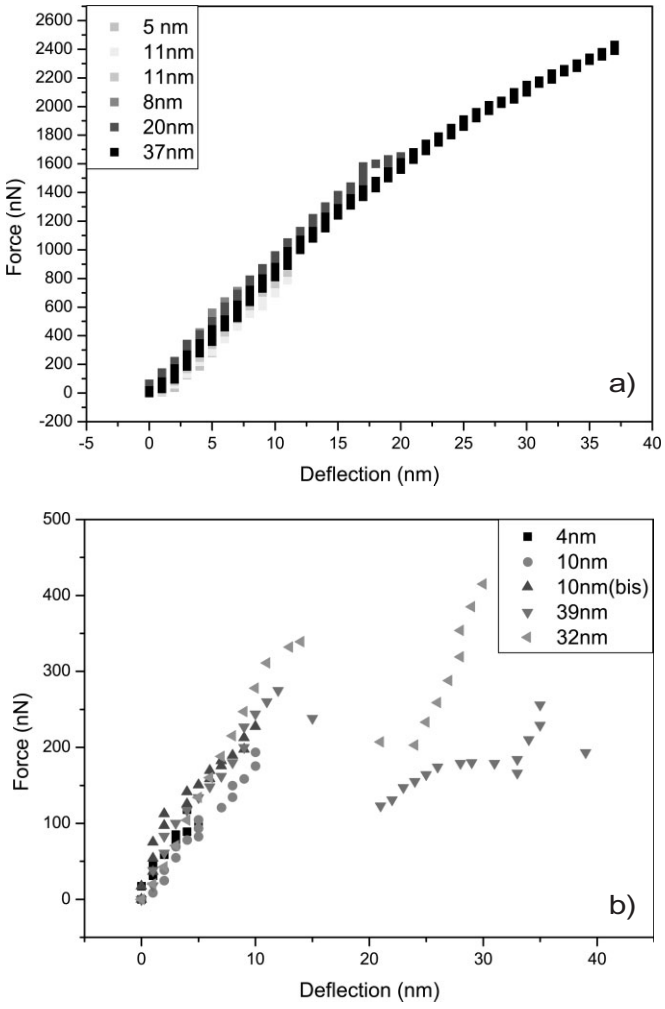

Figure 8. Force-deflection curves obtained by varying the nanotube's deflection: a) stoichiometric nanotubes; b) nanotubes doped with iron. The chrysotile nanotubes were dispersed in distilled water with added polyvinyl pirrolidone. The lengths in the figure legends refer to the maximal deflec-

Table 3. Young's modulus and standard deviation of stoichiometric synthetic chrysotile nanotubes suspended in ethanol or in surfactant (polyvinyl pirrolidone).

Stoichiometric synthetic chrysotile	Suspension solution	Young's modulus [GPa]	Standard deviation [GPa]
1 wall	ethanol	142	90
2 walls	ethanol	147	134
3 walls	ethanol	85	0
2 walls	surfactant	159	125

sotile nanotubes is (159±125) GPa and (279±260) GPa, respectively. Nanotubes with outer diameter ranging from (22 to 28) nm are presumed to be single wall nanotubes. In contrast with the usual definition of a single wall nanotube, which is made of an individual molecular layer, like carbon or WS_2, here a typical wall consists of 5–7 monomolecular OT sheets.[27] On the other hand nanotubes with an outer diameter ranging from (32 to 38) nm and (40 to 48) nm are estimated to be composed of two and three concentric walls, respectively.[27] The determined Young's modulus of the stoichiometric and Fe doped synthetic chrysotile nanotube are reported as a function of the number of walls in Tables 3 and 4, respectively. Notwithstanding the limited number of measured nanotubes the mechanical behavior of the nanotubes seems to be closely related to the number of the constituting walls (recall that each wall consists of 3–4 OT molecular layers). It appears that the Young's modulus values decrease when the number of walls increases, suggesting that multiwall nanotubes have relative larger amount of structural defects compared with singlewall nanotubes. Further quantitative work is needed to establish the relationship between the diameter of the nanotubes and their elastic constants. Structural defects; loose contact of the nanotube to the underlying GaAs surface; a non-perpendicular alignment of the nanotube with respect to the trenches, can all

Table 4. Young's modulus and standard deviation of 0.67 wt % Fe doped synthetic chrysotile nanotubes suspended in ethanol or in surfactant (polyvinyl pirrolidone).

0.67% Fe doped synthetic chrysotile	Suspension solution	Young's modulus [GPa]	Standard deviation [GPa]
1 wall	ethanol	560	110
2 walls	ethanol	224	157
3 walls	ethanol	74	0
2 walls	surfactant	583	128
3 walls	surfactant	97	50

affect the calculated values of the Young's modulus. Nevertheless, the average Young's modulus of the stoichiometric chrysotile is in good agreement with the value reported for naturally occurring chrysotile fibers in the range of 158–185 GPa[32–34] (the highest value was obtained from atomistic calculations). The good agreement between the atomistic calculations and the measured values suggest that the naturally occurring impurities have little influence on the Young's modulus of the chrysotile nanotubes. Notwithstanding the large scatter of the present experimental data, the average Young's modulus of the Fe-doped chrysotile nanotubes is almost twice as large as that of stoichiometric chrysotile nanotubes. This observation may be the result of structural modifications caused by the Fe doping as was observed by the TEM analysis. Furthermore, according to the XRD analysis, the degree of chrysotile crystallinity falls with increasing inclusion of Fe in the synthesized phase. The Fe substitution in chrysotile may reduce the mismatch between the $Mg(OH)_2$ and Si_2O_5 layers thus lowering the elastic strain and resulting in a flatter morphology. It may also induce host–guest charge transfer, leading to strengthening of the 3D character and reduced anisotropy of the lattice. The determination of the Young's modulus is based on the hypothesis that the entire load is taken by the outermost wall, only. This model appears to be valid to the tensile tests of materials with highly anisotropic nature, like graphite, or MoS_2, but is certainly not applicable for the bending of beams of 3D nature. Therefore, this model may provide an overestimate for the Young's modulus of the Fe-doped chrysotile nanotubes which are more 3D in nature as a result of its defects and the guest-host charge transfer.

3. Conclusions

Synthetic chrysotile nanotubes, both stoichiometric and Fe doped were mechanically characterized by performing bending tests. Linear elastic behaviour was observed for small deformations (in the range of 15–20 nm). Some of the nanotubes failed, and fracture occurred at large deflections of 100–150 nm. Furthermore, the Young's modulus was calculated from the force-deflection curves using the bending equation. Values of (159 ± 125) GPa and (279 ± 260) GPa were obtained for stoichiometric chrysotile and Fe doped nanotubes, respectively. The Young's modulus data suggests that the mechanical behavior of the nanotubes is possibly related to the number of the walls (each wall consisting of 5–7 OT layers) constituting the sample. The Young's modulus of the stoichiometric synthetic nanotubes is in good agreement with the value of natural chrysotile fibres which are usually heterogeneously doped with many foreign metallic ions. Structural modifications of the nanotubes by Fe doping were shown to alter its mechanical properties as well.

4. Experimental

Stoichiometric Synthetic Chrysotile: A modification of the synthesis method reported by Falini et al. [28] was used to synthesize stoichiometric chrysotile nanotubes. A hydrothermal synthesis reactor (Parr Stirred "Mini" reactor model 4564 with moveable vessel styles) with a 160 cm^3 vessel was used to carry out the hydrothermal reaction of SiO_2 and $MgCl_2$ in an aqueous NaOH (0.4 M) solution. The reactants used were Aerosil 380 in the form of a powder with a surface area of about 380 $m^2 g^{-1}$ (Eigenmann & Veronelli S.p. A). The hydrothermal treatment was carried out at a temperature of 300 °C on the saturated vapour pressure curve (82 atm) with a run duration of 24 h. The precipitate removed from the solution was repeatedly washed with deionised water and dried for 3 h at 150 °C.

Fe-Doped Synthetic Chrysotile: The Fe doped chrysotile nanotubes were synthesized according to the method reported by Foresti et al. 2005 [31]. A gel mixture of SiO_2, $FeCl_3$ and $MgCl_2$ with a Si/Mg+Fe molar ratio of 0.68, in an aqueous solution was prepared. An Fe/Fe+Mg molar ratio of 1.50 % was used. The pH of this mixture was raised to the range 12–13 by means of an aqueous NaOH (0.4 M) solution. The hydrothermal treatment was carried out at a temperature of 300 °C, where according to the saturated vapour pressure curve the pressure attains 82 atm. The reaction was run from 8 h to 3 days. The precipitate removed from the solution was repeatedly washed with deionized water before being dried for 3 h at 150 °C. 0.66 wt % Fe content has been determined in the synthesized iron doped nanotubes by inductively coupled plasma atomic emission spectrometry (ICP-AES) analysis, using a Varian Liberty Model 200 analyzer.

Morphological Investigations: Morphological characterization of the nanotubes was carried out by TEM. The powdered material was suspended in doubly distilled water and then a drop of the suspension was dripped on carbon/collodion foils supported on conventional copper grids. TEM model CM-120 operated at 120 kV equipped with energy dispersive spectrometer (EDAX-Phoenix Microanalyzer) was used for the present analysis. TEM studies were carried out under low dose conditions, due to the beam sensitivity of the specimens which can lead to disappearance of the crystallinity.

Bending Tests: In the present study, bending tests of chrysotile nanotubes were performed using the AFM according to a previously published procedure [3,21]. This procedure involves lateral manipulation of an individual nanotube which is mechanically fixed to and positioned over trenches on a GaAs substrate (Fig. 7). Trenches were fabricated by electron beam lithography to be 0.5–0.6 μm wide and 200–300 nm deep. The chrysotile nanotubes were dispersed in an appropriate solvent for 30 s and suspended over the GaAs substrate. Different solvents (acetone, distilled water, ethanol and polyvinyl pirrolidone water solution) have been used in order to form a stable chrysotile nanotubes suspension. The dispersed nanotubes were mapped with a high resolution scanning electron microscope (HRSEM). The resulting structures were subjected to lateral loading by an AFM cantilever under closed-loop control. With the tip cruising 70–100 nm above the plane of the substrate, the lateral deflection of the cantilever was monitored during the manipulation and the corresponding F-d trace was recorded. Following the deflection test, each nanotube was imaged both by AFM and SEM to search for any morphological variation. The raw deflection data was separated into the cantilever torsional deflection and the nanotube deflection (the canti-

ADVANCED FUNCTIONAL MATERIALS

lever torsional force constant was calibrated according to Sader's torsional method [35]).

Received: March 7, 2007
Revised: May 2, 2007
Published online:

[1] M. F. Yu, O. Lourie, M. J. Dyer, K. Moloni, T. F. Kelly, R. S. Ruoff, *Science* **2000**, *287*, 637.
[2] A. H. Barber, I. Kaplan-Ashiri, S. R. Cohen, R. Tenne, H. D. Wagner, *Compos. Sci. Technol.* **2005**, *65*, 2380.
[3] B. Wu, A. Heidelberg, J. J. Boland, *Nat. Mater.* **2005**, *4*, 525.
[4] I. Kaplan-Ashiri, S. R. Cohen, K. Gartsman, V. Ivanovskaya, T. Heine, G. Seifert, I. Wiesel, H. D. Wagner, R. Tenne, *Proc. Natl. Acad. Sci. USA* **2006**, *103*, 523.
[5] B. I. Yakobson, P. Avouris, *Carbon Nanotubes* **2001**, *80*, 287.
[6] I. Kaplan-Ashiri, S. R. Cohen, K. Gartsman, R. Rosentsveig, G. Seifert, R. Tenne, *J. Mater. Res.* **2004**, *19*, 454.
[7] J. Cumings, A. Zettl, *Science* **2000**, *289*, 602.
[8] B. G. Demczyk, Y. M. Wang, J. Cumings, M. Hetman, W. Han, A. Zettl, R. O. Ritchie, *Mater. Sci. Eng. A* **2002**, *334*, 173.
[9] J. Y. Huang, S. Chen, Z. Q. Wang, K. Kempa, Y. M. Wang, S. H. Jo, G. Chen, M. S. Dresselhaus, Z. F. Ren, *Nature* **2006**, *439*, 281.
[10] Z. L. Wang, P. Poncharal, W. A. de Heer, *J. Phys. Chem. Solids* **2000**, *61*, 1025.
[11] A. H. Barber, S. R. Cohen, S. Kenig, H. D. Wagner, *Compos. Sci. Technol.* **2004**, *64*, 2283.
[12] A. H. Barber, S. R. Cohen, H. D. Wagner, *Appl. Phys. Lett.* **2003**, *82*, 4140.
[13] C. A. Cooper, S. R. Cohen, A. H. Barber, H. D. Wagner, *Appl. Phys. Lett.* **2002**, *81*, 3873.
[14] J. M. Gere, *Mechanics of Materials*, 6th ed., Brooks/Cole, Pacific Grove, CA **2004**.
[15] S. Timoshenko, *Strength of Materials*, 3rd ed., Van Nostrand Reinbold, New York **1955**.
[16] H. D. Wagner, S. Fischer, I. Roman, G. Marom, *Composites* **1981**, *12*, 257.
[17] H. D. Wagner, G. Marom, I. Roman, *Fibre Sci. Technol.* **1982**, *16*, 61.
[18] J. P. Salvetat, G. A. D. Briggs, J. M. Bonard, R. R. Bacsa, A. J. Kulik, T. Stockli, N. A. Burnham, L. Forro, *Phys. Rev. Lett.* **1999**, *82*, 944.
[19] A. Kis, D. Mihailovic, M. Remskar, A. Mrzel, A. Jesih, I. Piwonski, A. J. Kulik, W. Benoit, L. Forro, *Adv. Mater.* **2003**, *15*, 733.
[20] I. Kaplan-Ashiri, S. R. Cohen, N. Apter, Y. Wang, G. Seifert, H. D. Wagner, R. Tenne, *J. Phys. Chem. C* **2007**, *111*, 8432.
[21] D. A. Walters, L. M. Ericson, M. J. Casavant, J. Liu, D. T. Colbert, K. A. Smith, R. E. Smalley, *Appl. Physi. Lett.* **1999**, *74*, 3803.
[22] K. Yada, *Acta Crystallogr.* **1967**, *23*, 704.
[23] K. Yada, *Acta Crystallogr.* **1971**, *27*, 659.
[24] E. Whittake, *Acta Crystallogr.* **1957**, *10*, 149.
[25] B. A. Cressey, E. J. W. Whittaker, *Mineral. Mag.* **1993**, *57*, 729.
[26] F. J. Wicks, D. S. Ohanley, *Rev. Mineral.* **1988**, *19*, 91.
[27] G. Falini, E. Foresti, M. Gazzano, A. E. Gualtieri, M. Leoni, I. G. Lesci, N. Roveri, *Chem. Eur. J.* **2004**, *10*, 3043.
[28] G. Falini, E. Foresti, G. Lesci, N. Roveri, *Chem. Commun.* **2002**, 1512.
[29] E. Gazzano, E. Foresti, I. G. Lesci, M. Tomatis, C. Riganti, B. Fubini, N. Roveri, D. Ghigo, *Toxicol. Appl. Pharmacol.* **2005**, *206*, 356.
[30] C. Bergamini, R. Fato, G. Biagini, A. Pugnaloni, F. Glantomassi, E. Foresti, G. I. Lesci, N. Roveri, G. Lenaz, *Cell. Mol. Biol.* **2004**, *50*, 691.
[31] E. Foresti, M. F. Hochella, H. Kornishi, I. G. Lesci, A. S. Madden, N. Roveri, H. F. Xu, *Adv. Funct. Mater.* **2005**, *15*, 1009.
[32] *Asbestos: Properties, Applications, and Hazards* (Eds: S. S. Chissick, R. Derricott), Vol. 2, Wiley, Chichester, UK **1983**.
[33] J. Aveston, *J. Mater. Sci.* **1969**, *4*, 625.
[34] A. L. Auzende, R. J. M. Pellenq, B. Devouard, A. Baronnet, O. Grauby, *Phys. Chem. Miner.* **2006**, *33*, 266.
[35] C. P. Green, H. Lioe, J. P. Cleveland, R. Proksch, P. Mulvaney, J. E. Sader, *Rev. Sci. Instrum.* **2004**, *75*, 1988.

FULL PAPERS

Inorganic Nanotubes

S. Piperno, I. Kaplan-Ashiri,
S. R. Cohen, R. Popovitz-Biro,
H. D. Wagner, R. Tenne,* E. Foresti,
I. G. Lesci, N. Roveri ..... ■ – ■

Characterization of Geoinspired and Synthetic Chrysotile Nanotubes by Atomic Force Microscopy and Transmission Electron Microscopy

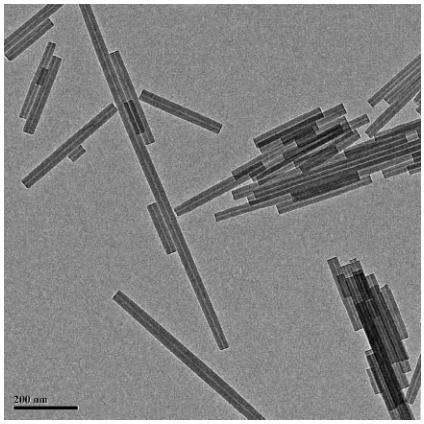

The structural and mechanical properties of geoinspired synthetic chrysotile nanotubes (see figure) are studied in both stoichiometric and 0.67 wt % Fe-doped forms. It is demonstrated that doping induces structural modifications and alters the Young's modulus value as well.